Influence of Suction on the Properties of two Granular Road Materials

Octavio Coronado & Jean-Marie Fleureau
Ecole Centrale Paris, Châtenay-Malabry, France

António Gomes Correia
Universidade do Minho, Guimarães, Portugal

Bernardo Caicedo
Universidad de los Andes, Bógota, Colombia

ABSTRACT: The results of an experimental work on two road granular materials are presented, including small strains precision triaxial tests under cyclic loading, large strains triaxial tests with measurement of the negative pore water pressure (suction) and wetting tests. The influence of different initial conditions of density, water content and fines content was studied. The two materials differ by their fine contents (7 % for MHC and 10% for HFC). The specimens are compacted at different water content and at a density corresponding to 97% of the Modified Proctor maximum density. The interpretation of the results, in the quasi-elastic domain, is based on an effective stress analysis that allows to take into account both the effects of total stresses and negative pressure, in the perspective of a more rational design of pavement layers.

KEYWORDS: Roads, unsaturated unbound materials, modulus

1 INTRODUCTION

In practice, pavement design is based on rational methods using Young' modulus (E) and Poisson's ratio ( ). These parameters are generally determined in terms of total stresses, even though the granular materials used in road construction are in an unsaturated state. In the laboratory, the negative pore water pressure, or suction (uc = ua - uw), is not easy to measure in coarse materials and their derivation requires the use of elaborate tests.

Several authors have studied the effect of the negative pore water pressure on the behavior in small distortions of partially saturated soils (Brull 1980, Wu and al. 1989, Kheirbek-Saoud 1994, Picornell and Nazarian 1998, Balay et al. 1998). In most cases, the analysis of the results is made in total stresses, and the role of the stress tensor is considered separately from that of the negative pore water pressure. Other authors (Wu and al. 1989, Biarez et al. 1991, Coussy & Dangla 2002, Fleureau et al. 2003) showed that an effective stress approach could be used to take in account the effect of the capillary pressure in the interpretation of the data in the very small strains domain.

In this study, both small and large strains triaxial tests with measurement of negative pore water pressure have been performed on two untreated unbound granular materials (U.G.M.) used as references in France for road works. The materials have been recomposed with two percentages of fines (10% and 7%), and compacted in the laboratory at different water contents, to a dry density corresponding to 97% of the Modified Proctor maximum density. Wetting tests have been carried out to determine suction and water content changes in the material during wetting. One of the goal of this paper is to show how to take moisture changes into account in the pavement design analysis using an effective stress approach.

2 MATERIALS AND METHODS

2.1 Materials

The materials used in this study are mainly composed of gneiss coming from the "Maraîchères" quarry in France. They are made from the mixture of five different fractions: 0/4 mm sand, 2/6,3 mm gravel, 4/10 mm gravel, 10/14 mm gravel and 14/20 mm gravel. The reference grain size distributions used in this study contain 7% and 10% of fine elements (<80 µm); they are called MGC and HFC, respectively. Figure 1 shows the grain size distribution curves and the compaction curves of the mixtures, determined in accordance with the French standards NFP 98-129 and NFP 94-093. The grain size distribution curves for the two materials fall inside the French specifications for road materials. The maxima of the compaction curves correspond to a water content (w_{MOP}) of 5,8% and a dry density of 2,2 Mg/m^3 for MGC, and a water content of 5.5% and a dry density of 2,22 Mg/m^3 for HFC. The value of the Los Angeles abrasion coefficient is approximately 20%.

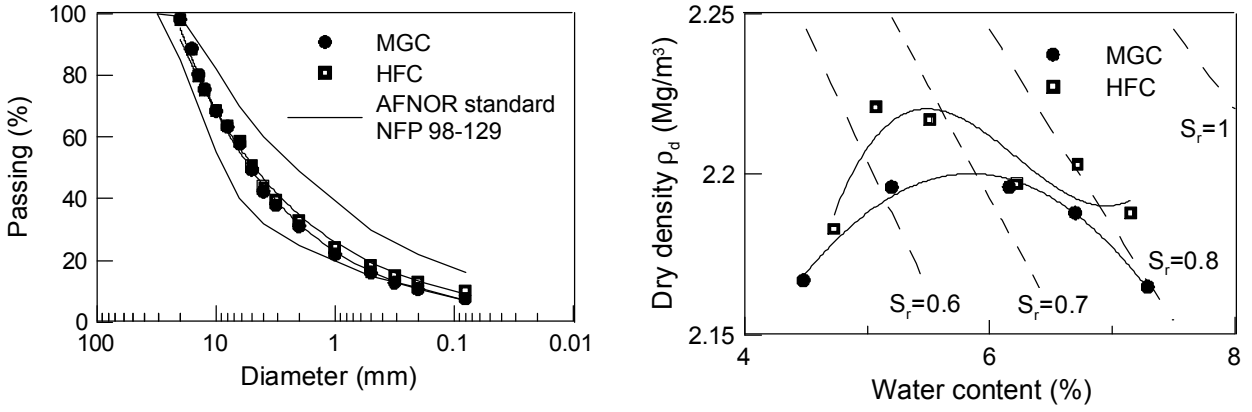

Figure 1: Grain size distribution and Proctor Modified compaction curves of the two soils

2.2 Cyclic triaxial tests

The cyclic tests were carried out in a classic triaxial cell, allowing a direct measurement of the stiffness modulus and Poisson's ratio for homogeneous strains ranging between 10^{-6} and 10^{-2}. To

be able to explore the domain of the very small strains with sufficient accuracy, the force and strain measurements are done on the specimen itself. The force transducer is placed inside the cell directly on the head of the specimen, which permits a precise measurement of the force applied to the specimen and eliminates the bearing-piston friction problems. The measure of the axial strains is achieved by means of three LDT strain sensors placed in the central zone of the specimen, in order to avoid the influence of the constrictions of the bases on the measures. Radial strains are derived from the variations of the perimeter of the specimen measured by a deformable belt placed to mid-height and equipped with a LDT sensor. The LDT sensors are constituted of 4 strain gauges forming a complete Wheatstone bridge fixed on a deformable blade made of beryllium bronze; they were manufactured at the Ecole Centrale Paris on the model of the sensors developed at the university of Tokyo in the team of Professor Tatsuoka (Goto et al. 1991). Supports for the sensors are put in place in the specimen during the compaction. The accuracy of the strain measurements is approximately 10^{-5} with a 21 bits Agilent A/D converter.

To prepare the specimens, water is added to the dry mixture in a homogenous way. Dynamic compaction of the specimen, 150 mm in diameter and 300 mm in height, is achieved by hand by means of a Modified Proctor rammer, in 12 layers with 56 strokes of rammer per layer. The initial properties of the specimens are shown in Table 1. During the manufacture of the specimens, special attention is paid to the setting up of the six supports of the vertical sensors. Then, the axial and radial strain sensors are put in place, as well as the force transducer.

Table 1. Initial conditions of the specimens for the small and large strains tests

		Dry density (Mg/m^3)	Water content (%)
Test 2	MGC	2.123	2.05
Test 3		2.132	3.86
Test 4		2.167	5.12
Test 5		2.132	2.00
Test 8	HFC	2.150	3.50

To determine the reversible behavior of the materials, preliminary conditioning of the specimens is carried out in order to simulate the real conditions of laying down of the soil: it consists in 20000 loading-unloading cycles under an isotropic stress of 40 kPa and a deviatoric stress of 280 kPa. After the pre-conditioning, the specimen is submitted to 20 successive paths with increasing levels of stress (Figure 2a). All the tests are made under constant confining stress σ_3. Each loading is applied during 100 cycles. The reversible strains of the specimen are measured during the 100th cycle. An example of the measurements is shown on Figure 2b, where the deviatoric stress q is represented versus the axial, radial and volumetric strains (ε_1, ε_3 and ε_v, respectively). These cycles illustrate the non linearity of the behavior, i.e. the increase in the modulus with q, when the axial strain exceeds the elastic limit of the material (about 10^{-5}).

The secant module is defined in the following way:

$$E_{sec} = q / \varepsilon_1^r \qquad [1]$$

The measurements are made for axial strain ε_1^r approximately equal to 10^{-4}.

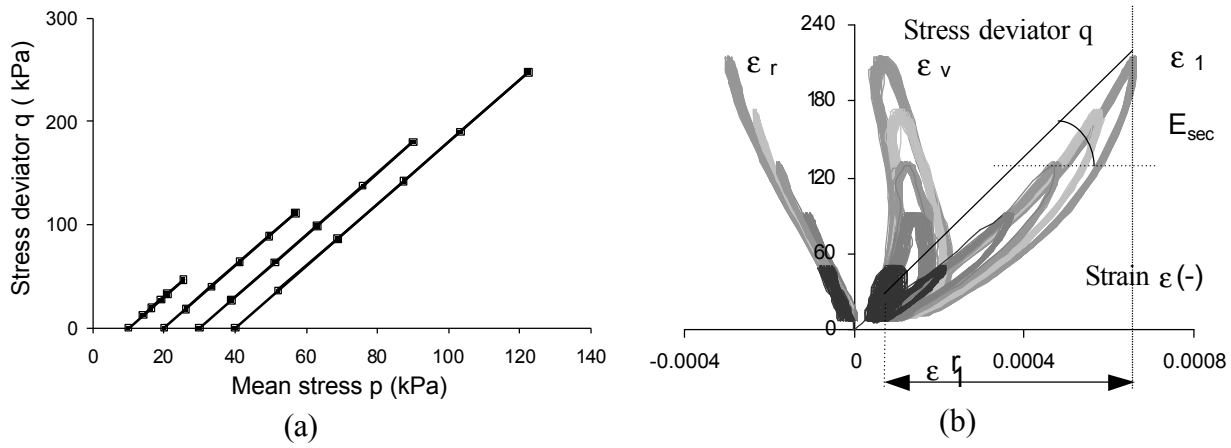

Figure 2: (a) Stress paths for the determination of the elastic properties of the materials and (b) example of measurement of the stress deviator vs. axial, radial and volumetric strains

2.3 Triaxial tests with measurement of the negative pore water pressure

The device consists of a triaxial cell with a semi-permeable ceramics placed in the base; the porous stone with high air entry pressure (1,5 MPa, from Soil Moisture) doesn't permit the passage of air in the water circuit. The device can be used either as a tensiometer (with $u_a = 0$ and $u_w < 0$) to measure negative pore water pressures between 0 and 50 kPa, or with an air overpressure at the head of the specimen for higher negative pressures. Pore water pressure measurements are done by means of an absolute pressure sensor with a range of 1000 kPa and a sensitivity of 0,1 kPa/mV. Data logging is achieved by means of a 16 bits GDS data acquisition system.

The size of the specimens is 100 mm in diameter and 200 mm in height. Specimens were dynamically compacted by means of a Modified Proctor rammer in 4 layers, with 56 strokes per layer. A thin layer of kaolinite is placed on the ceramics to ensure a good contact with the specimen and the continuity of the water phase. The measures have been made in the conditions of tests 3 (MGC material, $w = w_{MOP} - 2\%$) and 8 (HFC material, $w = w_{MOP} - 2\%$).

2.4 Wetting tests on tensiometric plates

To impose negative pore water pressures ranging between 0 and 30 kPa, tensiometric plates were used. They are made of a a low porosity sintered glass filter, that plays role of the semi-permeable separation, set in a glass funnel. The specimen is placed on the filter to the atmospheric pressure, in contact with a reservoir filled with de-aired water. Imposing a difference of level between the filter and the measurement tube results in controlling the depression of the water placed in the reservoir, and therefore the negative pore water pressure in the specimen.

At the end the cyclic triaxial tests, the specimen is cut into several pieces, that are placed on the tensiometric plate. The exchanges of water between the specimen and the reservoir are derived from the displacement of the water meniscus in a horizontal measurement tube connected to the reservoir. When the negative pore water pressure in the specimen reaches the imposed value, generally at the end of 5 days, the total volume of the specimen and its water content are derived

from immersion in kerdane followed by drying in an oven; the water content, void ratio and degree of saturation of the material are derived from these data.

3 RESULTS

3.1 Isotropic compression tests with measurement of pore water pressure

Figure 3a shows the non linear increase in pore water pressure u_w versus the isotropic stress σ_3 for the two grain size distributions. The pressure increases up to a value close to 0 under the highest stress (300 kPa) but, even in the initial state, suction values remain unimportant ($-u_w < 35$ kPa). Under the same isotropic stress, the negative pore water pressure is slightly higher in the case of the material with the highest percentage of fines (HFC), but both curves tend towards the same value when the isotropic stress reaches 300 kPa.

3.2 Wetting tests on the tensiometric plate

Figure 3b shows the results of the wetting tests, starting from the initial conditions indicated in Table 1. The shape of the negative pore water pressure versus water content curves presents the usual aspect. For the material with the highest percentage of fines, there is a slight shift of the wetting curve towards higher water contents (under the same suction) after the air entry point. This point, that corresponds to the negative pressure for which occurs the fast reduction of the degree of saturation and the water content, can be situated between 1 and 5 kPa for the two materials. One can note the good agreement between the suction values found in the triaxial tests with measurement of negative pore water pressure under $\sigma_3 = 0$ ("Test 3" and "Test 8" on Fig. 3b) and the wetting tests.

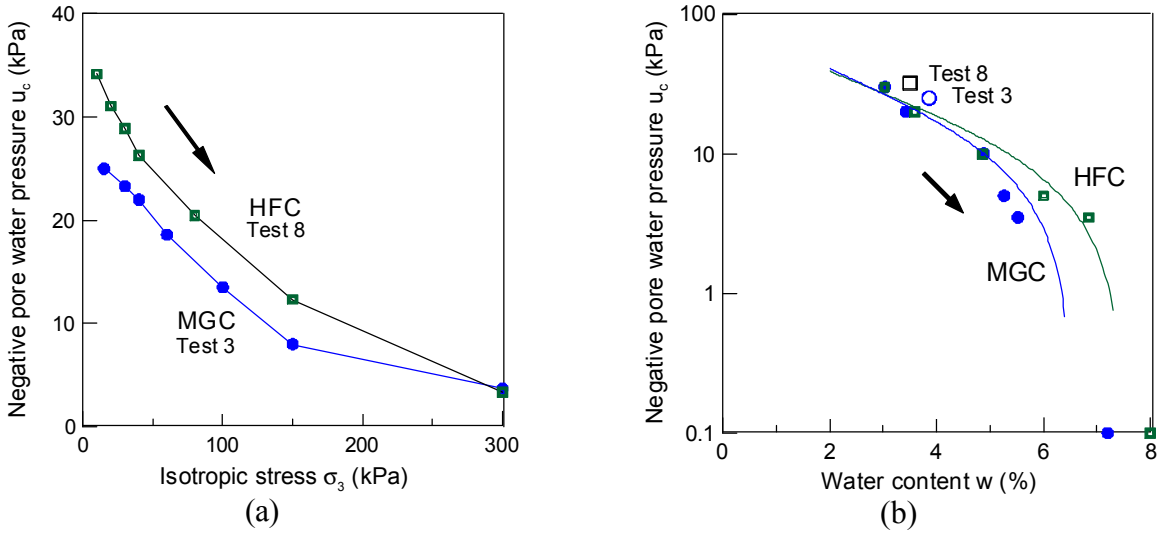

Figure 3. Changes in the negative pore water pressure according to (a) isotropic stress and (b) water content for the two materials

3.3 Small strains triaxial tests

Figure 4a shows the variation of the secant modulus of the MGC material as a function of the vertical stress, for different water contents ranging from 2% for tests n° 2 and 5 to 5.1% for test n° 4. One notes the sensitivity of the material to this parameter: under the same isotropic stress, the modulus is higher when the water content is smaller because of the increase in the capillary forces in the menisci that form themselves between the grains. As previously noted (Fleureau et al. 2003), the lines are more or less parallel for the different wet soils.

Figure 4b shows the variation of the secant module with the vertical stress σ_v for the two studied percentages of fines. When the percentage grows from 7% to 10%, the module noticeably increases. However, the influence of the dry density of the material, which is noticeably higher for HFC, compared to MGC (2.150 for test 8 against 2.132 for test 3), must be taken into account in the comparison.

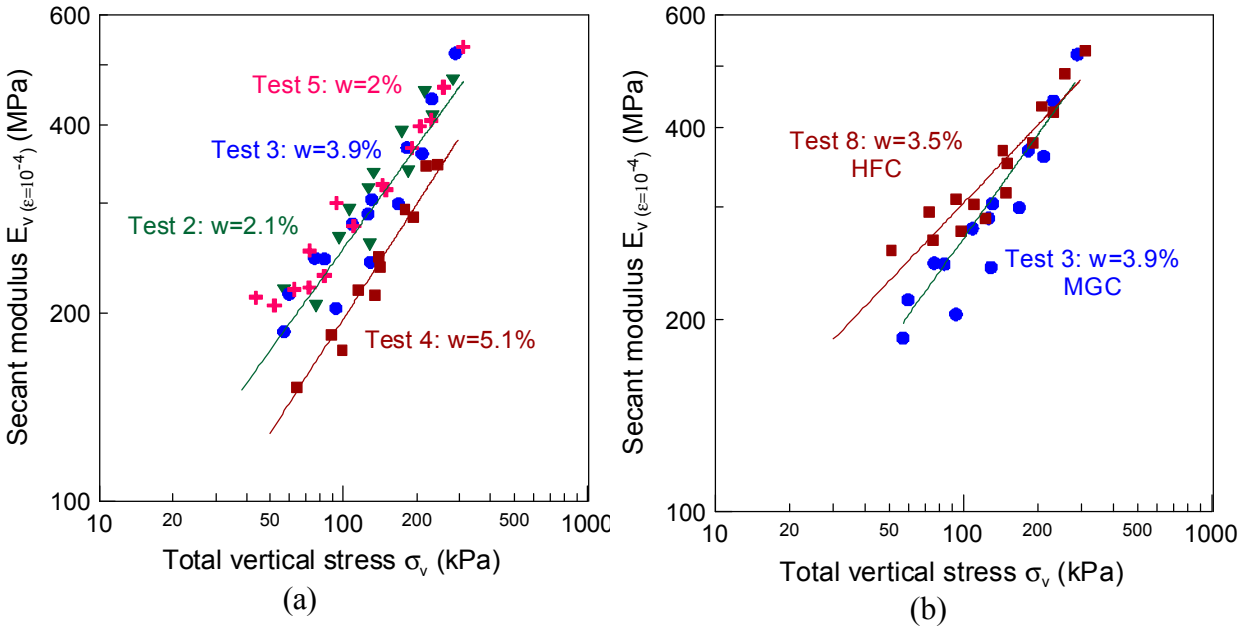

Figure 4. Influence of (a) the water content and (b) the percentage of fines on the secant modulus (for an axial strain of 10^{-4})

3.4 Large strains triaxial tests

Figure 5 shows the results of the large strains triaxial tests in different corresponding coordinate systems: Stress deviator q versus axial strain ε_1 and mean stress p, pore water pressure u_w versus axial strain and void ratio e versus axial strain and mean stress (both in normal and log scales).

In the [ε_1, q] coordinate system, the curves for the MGC material are classified according to the confining stress. They all present a peak, representative of an overconsolidated behaviour, usual in granular materials under low stresses. There is a small difference in the values of the maximum deviators between the two materials, under σ_3 = 0.3 MPa, but the large strains value are similar. In both [ε_1, u_w] and [ε_1, e] planes, the behaviour of the materials is clearly first con-

tractant, then dilatant for larger strains. The variations of the void ratio are small, probably because the materials are not very far from saturation, as evidenced by the values of the pore water pressure ranging between –20 and +5 kPa.

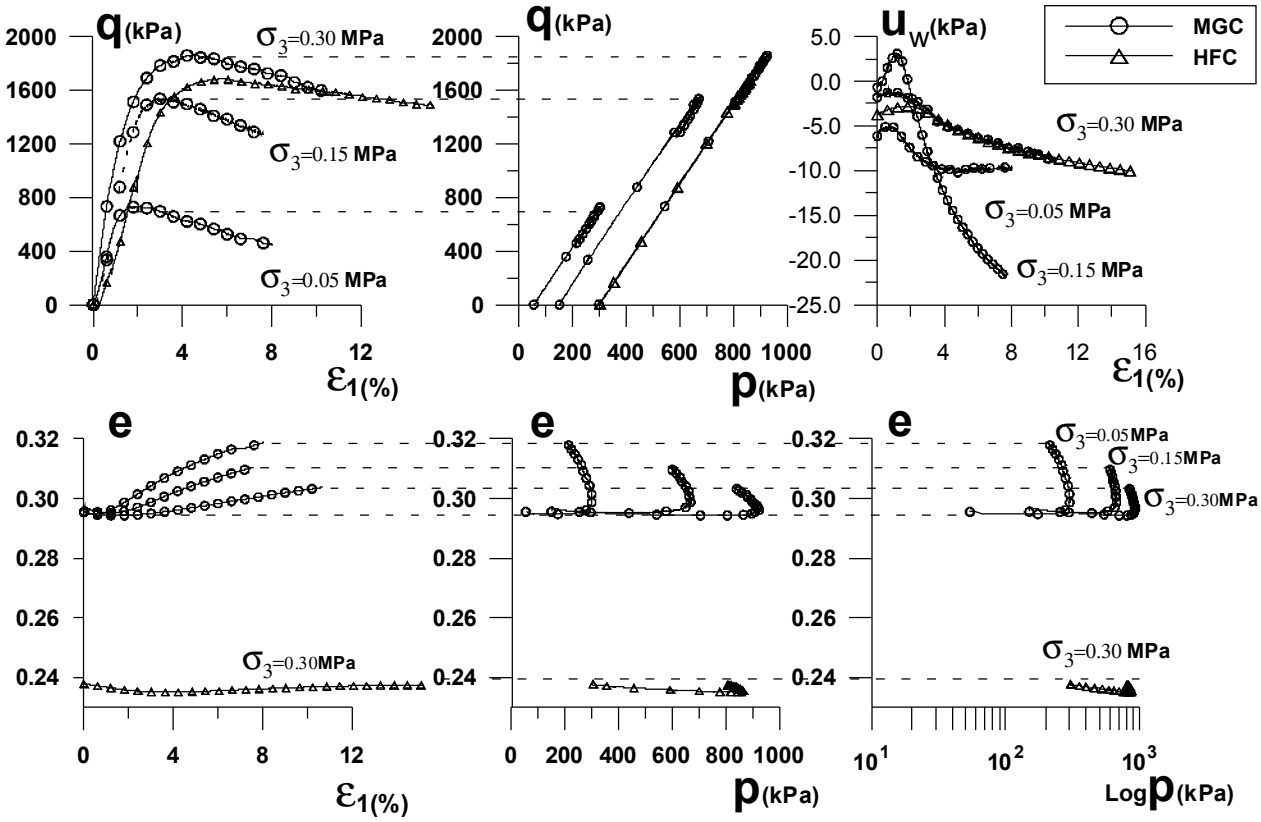

Figure 5: Results of large strains triaxial tests with measurement of negative pore water pressure for the two materials

4 INTERPRETATION OF THE RESULTS IN EFFECTIVE STRESSS

4.1 Taibi (1994)'s microstructural model for the calculation of the effective stress in unsaturated materials

Different expressions have been proposed to calculate the effective stress in an unsaturated medium. In the case of high negative pore water pressures and low degrees of saturation, the approach developed at the Ecole Centrale Paris is based on a micromechanical model composed of regular arrangements of non-deformable balls of the same diameter d (Fleureau et al. 2003). The increase in negative pore water pressure due to the reduction of the degree of saturation leads to an increase in the intergranular forces, which increases the moduli and the shear strength of the soil. For a regular arrangement of spheres, an elementary calculation based on Laplace's law results in the following expression of the capillary stress p'_u, that represents the contribution of the negative pore water pressure to the cohesion of the material. The capillary stress is a function of

suction and of the diameter d. In the case of a real grain size distribution, the parameter d must be determined. In the case of the materials tested, a previous analysis showed that the value d = 45 µm could be successfully used (Coronado et al. 2004). The expression to pass from total stresses to effective stresses is therefore:

$$\sigma'_v = \sigma_v + p'_u \quad [2]$$

4.2 Effective stress interpretation of the results at different water contents

Figure 6a represents the variations of the secant modulus versus the effective vertical stress for the two materials and the different water content conditions. To compare the results of the tests on the two materials, carried out at void ratios of 0.30 and 0.21, respectively for MGC and HFC, it is necessary to normalise the moduli to the same value of void ratio. The relation of Iwasaki et al. (1978) was used to bring the moduli back to a void ratio of 0.3:

$$E_{v(e=0.3)} = E_{vo(e)} \cdot \frac{f(0.3)}{f(e)}, \text{ avec } f(e) = \frac{(1.93-e)^2}{(1+e)} \quad [3]$$

The effective stresses were derived from Taibi's model with d = 45 µm. The curves for the two materials are practically superimposed, which shows that, in this particular case, the grain size distribution only plays a role in the behavior of the material through the variations of the negative pore water pressure. The points for the various water contents regroup well around a unique straight line with equation:

$$\frac{E_v}{p_a} = 2404 \cdot \left(\frac{\sigma'_v}{p_a} \right)^{0.54} \quad [4]$$

where p_a is the atmospheric pressure.

Using the same approach and the same value of the parameter d (d = 45 µm), the points corresponding to the maxima of the stress deviator for the different large strains triaxial tests have been plotted on Figure 6b versus the effective mean stress. The different points are correctly located on straight lines passing through the origin, with slightly different slopes for the two materials. The cohesion and friction angle of the corresponding failure criteria are therefore:

- c = 0 and $\phi = 50°$ for MGC
- c = 0 and $\phi = 48°$ for HFC

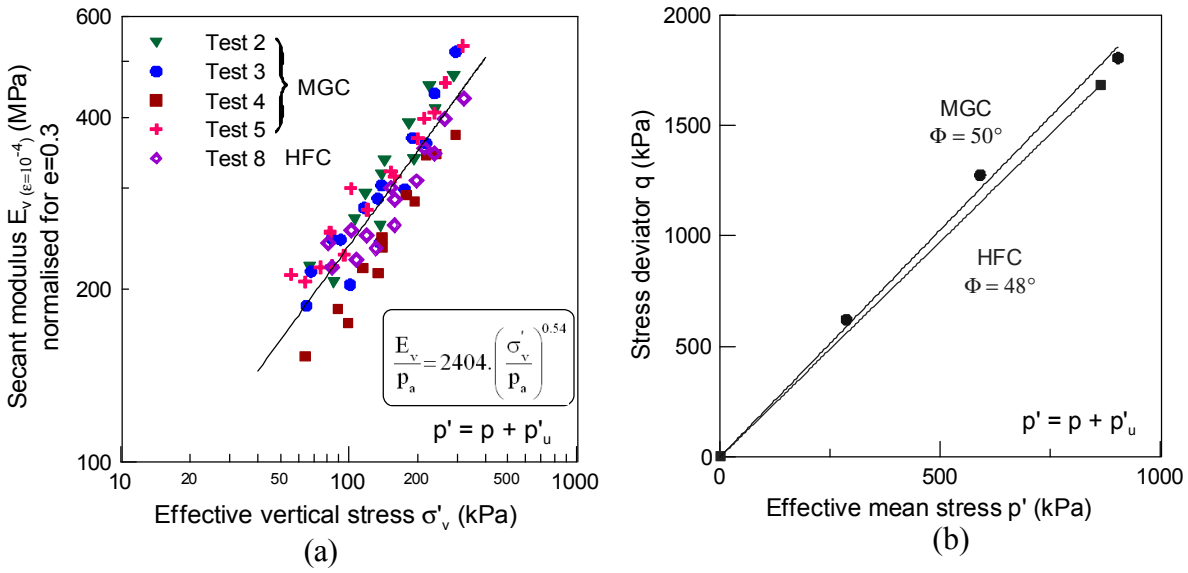

Figure. 6. (a) Variation of the normalised secant modulus with the vertical effective stress derived from Taibi's relation (for d = 45 µm) and (b) Failure criteria of the two materials in effective stresses (for d = 45 µm)

5 CONCLUSIONS

The precision triaxial tests performed on two road unbound granular materials highlight the non linear behavior of the materials. The effect of the water content on the secant modulus and strength is important. The interpretation of the results in terms of effective stresses based on suction measurements and the use of a simple micromechanical model show that it is possible to take into account the effect of water content on the reversible parameters and the failure criterion. The role of the grain size distribution appears rather limited in the case of the two studied materials and seems limited to a change of suction.

These results permit to generalise the constitutive laws developped for dry untreated unbound granular materials to larger conditions of water content, representative of the real conditions in the pavements.

REFERENCES

Balay, J., Gomes Correia, A., Jouve, P., Hornych, P. & Paute, J. 1998 *Etude expérimentale et modélisation du comportement mécanique des graves nos traitées et des sols support de chaussées*, Bull. Ponts & Ch., 216 : 3-18.

Biarez, J., Fleureau, J.M. & Kheirbek-Saoud, S., 1991. *Validité de* s'=s - u_w *dans un sol compacté*, 10th E.C.S.M.F.E., Firenze, Vol. 1: 15-18.

Brull A. 1980. *Caractéristiques mécaniques des sols de fondation de chaussées en fonction de leur état d'humidité et de compacité*, Coll. Int. Compactage, Presses Ponts & Chaussées, Paris, Vol. 1: 113-118.

Coronado O., Caicedo B., Fleureau J.-M. & Gomes Correia A. 2004. *Influence de la succion sur les propriétés d'un matériau granulaire routier*, Compte-rendus du 57ème Congrès Canadien de Géotechnique « GeoQuébec2004 », Québec, Canada, 24-28 Octobre 2004.

Coussy, O. & Dangla, P. 2002. *Approche énergétique du comportement des sols non saturés*, in Mécanique des sols non saturés, Hermès, Paris : 137-174.

Goto, S., Tatsuoka, F., Shibuya, S., Kim Y.-S. & Sato, T. 1991. *A simple gauge for local small strain measurements in the laboratory*, Soils and Foundations, 31, 1 : 169-180.

Fleureau, J.-M., Hadiwardoyo, S. & Gomes Correia, A 2003. *Generalised effective stress analysis of strength and small strains behaviour of a silty sand, from dry to saturated state*, Soils and Foundations, 43, 4 : 21-33.

Iwasaki, T., Tatsuoka, F. and Takagi, Y. 1978. *Shear Moduli of Sands under Cyclic Torsional Shear Loading*, Soils and Foundations, **18**, 1: 39-50.

Kheirbek-Saoud, S. 1994. PhD Thesis, Ecole Centrale Paris

Picornell, M. & Nazarian, S. 1998. *Effects of soil suction on the low-strain shear modulus of soils*, 2nd Int. Conf. on Unsat. Soils, Beijing, 2: 102-107.

Taibi, S. 1994. PhD Thesis, Ecole Centrale Paris.

Wu, S., Gray, D.H. & Richart, F.E. 1989. *Capillary effects on dynamic modulus of sands and silts*, Geot. Eng. Div. J., ASCE, 110 (9): 1188-1203.